

Toward the Neurocomputer: Image Processing and Pattern Recognition With Neuronal Cultures

Maria Elisabetta Ruaro, Paolo Bonifazi, and Vincent Torre*

Abstract—Information processing in the nervous system is based on parallel computation, adaptation and learning. These features cannot be easily implemented on conventional silicon devices. In order to obtain a better insight of how neurons process information, we have explored the possibility of using biological neurons as parallel and adaptable computing elements for image processing and pattern recognition. Commercially available multielectrode arrays (MEAs) were used to record and stimulate the electrical activity from neuronal cultures. By mapping digital images, i.e., arrays of pixels, into the stimulation of neuronal cultures, a low and bandpass filtering of images could be quickly and easily obtained. Responses to specific spatial patterns of stimulation were potentiated by an appropriate training (tetanization). Learning allowed pattern recognition and extraction of spatial features in processed images. Therefore, neurocomputers, (i.e., hybrid devices containing man-made elements and natural neurons) seem feasible and may become a new generation of computing devices, to be developed by a synergy of Neuroscience and Material Science.

Index Terms—Long-term potentiation, multielectrode array, neuronal culture, pattern recognition.

I. INTRODUCTION

UNDERSTANDING differences and similarities between conventional computers and biological nervous systems is a fascinating problem, at the core of Neuroscience and Computer Science. This comparison can provide a deeper understanding of human intelligence and may pave the way to the design of new computing devices. Standard silicon devices solve serial problems very efficiently, but, despite their remarkable speed, are less suitable for solving the parallel problems of artificial intelligence, computer vision and robotics [1], [2]. Because of the difficulty of forming large numbers of interconnections, man-made devices are not ideal for massive parallel processing, a task for which biological neurons are very suitable. Biological neurons form connections and synapses between themselves very naturally. Despite being slow and often unreliable computing elements [3]–[5], neurons operate extremely well in parallel and can adapt and learn.

In order to capture basic computational properties of biological neuronal networks, artificial neural networks (ANNs) were developed [1], [2]; [6]–[8]. ANNs can be trained to recognize features and patterns. However, ANNs are usually implemented on conventional serial machines thereby losing their biological

inspiration. Their implementation on genuinely parallel devices, ideally networks of natural neurons that are able to learn, is certainly desirable.

The major aim of the present manuscript is to explore the possibility of using biological neurons as computing elements in a task commonly solved by conventional silicon devices: image processing and pattern recognition.

Advances in the biocompatibility of materials and electronics have allowed neurons to be cultured directly on metal or silicon substrates, through which it is possible to stimulate and record neuronal electrical activity [9]–[16]. The work here described shows that by using commercially available multielectrode arrays (MEAs), it is possible to process simple patterns using two fundamental properties of natural neuronal networks: parallelism and learning. By mapping digital images into the extracellular stimulation of the neuronal culture (in a one to one correspondence between pixels and electrodes) a low-pass filtering of the images is obtained. This processing occurs in just few milliseconds, independently from the dimension of the image processed. In addition, neuronal cultures can be trained to potentiate the response to a simple spatial pattern, due to changes in synaptic efficacy or long-term potentiation (LTP) [17], [18]. Therefore, the neuronal culture can be trained to recognize simple spatial patterns. Moreover filtering and learning can be combined to extract features from processed images.

These results show that biological neurons can be effectively used as computing elements for massively parallel problems and support the feasibility of neurocomputers, i.e., hybrid devices composed of biological neurons and artificial elements.

II. METHODS

A. Neuronal Culture Media

Dissection Medium: Hanks' modified $-Ca^{2+}/Mg^{2+}$ free-resolution supplemented with 4.2 mM $NaHCO_3$, 12 mM Hepes, 33 mM D-glucose, 200 μM kynurenic acid, 25 μM DL-2-amino-5phosphonovaleric acid (APV), 5 $\mu g/ml$ gentamycin, 0.3% BSA.

Digestion Medium: 137 mM NaCl, 5 mM KCl, 7 mM Na_2HPO_4 , 25 mM Hepes, 4.2 mM $NaHCO_3$, 200 μM kynurenic acid, 25 μM APV).

Culture Medium: Minimal Essential Medium with Earle's salts (GIBCO-Brl) supplemented with 5% fetal calf serum, 0.5% D-glucose, 14 mM Hepes, 0.1 mg/ml apo-transferrin, 30 $\mu g/ml$ insulin, 0.1 $\mu g/ml$ d-biotin, 1 mM Vit. B12 and 2 $\mu g/ml$ gentamycin.

B. Neuronal Dissection and Dissociation

The hippocampus from three-day-old Wistar rats was dissected in ice-cold dissection medium. Slices, were cut with a

Manuscript received October 17, 2003; revised August 5, 2004. This work was supported in part by the EU under Grant INPRO and in part by a FIRB grant from the Italian Ministers. *Asterisk indicates corresponding author.*

M. E. Ruaro and P. Bonifazi are with the INFN section and International School for Advanced Studies, I-34014 Trieste, Italy

*V. Torre is with the International School for Advanced Studies (SISSA), Via Beirut 2-4, 34014 Trieste, Italy (e-mail torre@sissa.it).

Digital Object Identifier 10.1109/TBME.2004.842975

razor blade, transferred in a 15-ml centrifuge tube and washed twice with the dissection medium. Slices were then treated with 5 mg/ml Trypsin and 0.75 mg/ml DNaseI in digestion medium for 5 min at RT to perform enzymatic dissociation. Trypsin was then neutralized by 1 mg/ml trypsin inhibitor in dissection medium for 15 min on ice. After three washes with the dissection medium, mechanical dissociation was performed by 10 passages through a P1000 blue tip. The cell suspension was then centrifuged at 100 g for 5 min, and pellet was re-suspended in culture medium.

C. MEA Coating

MEA dishes were coated by overnight incubation at 37 °C with 1 ml of 50 $\mu\text{g}/\text{ml}$ polyornithine (in water). Dishes were then air-dried and a film of BD-Matrigel (Beckton–Dickinson) was added on the electrode matrix region 20 min before seeding.

D. Cell Culture

100 μl of cell suspension was laid on the electrode array of precoated MEA at the concentration of 8×10^5 cells/cm². Cells were let to settle at room temperature for 20 min, and then 1 ml of culture medium was added to the MEA and incubated in a 5% CO₂ atmosphere at 37°C. After 48 hours 5 μM cytosine- β -D-arabinofuranoside (Ara-C) was added to the culture medium, in order to block glial cell proliferation, and re-incubated with gentle rocking.

E. Maintenance of Neuronal Cultures

Neuronal cultures were kept in an incubator providing a controlled level of CO₂ (5%), temperature (37°C) and moisture (95%). Half the medium was changed twice a week. Recordings were performed, in culture medium, from 3 weeks after seeding for up to 3 months. To decrease water evaporation and to maintain sterile conditions outside the incubator [19], during electrical recordings dishes were sealed with a cap manufactured by ALA Science and distributed by MCS (MultiChannelSystem). After termination of the experiment, usually after 3 to 10 hours, the cap was removed, the medium was changed and the dish was moved back to the incubator. The same dish could be used for other experiments in the following days and often repetitively over a month. In some cases the same dish was used for more than four different experiments.

F. Electrical Recordings and Electrode Stimulation

MultiChannelSystems commercially supplied the MEA system used for electrical recording. We used a 10×6 microelectrode array, with 500 μm spacing between adjacent electrodes. Each titanium-nitride microelectrode has a 30 μm diameter circular shape; its frequency-dependent impedance is of the order of 100 k Ω at 1 kHz. Through gold contacts it is connected to a 60 channel, 10 Hz –3 kHz bandwidth preamplifier/filter-amplifier (MEA 1060-AMP) which redirects the signals toward a further electronic processing (i.e., amplification and AD conversion), operated by a board lodged within a high performance PC. Signal acquisitions are managed under software control. A thermostat (HC-X) maintains the temperature at 37 °C underneath the MEA. The MEA provided by MCS is able to digitize in real time at 20 kHz all voltage recordings obtained from the 60 metal electrodes. One electrode was

used as ground [see Fig. 1(c)]. Sample data were transferred in real time to the hard disk for later processing. Each metal electrode could be used for recording or for stimulation, but the present MCS system does not allow a computer-controlled switch from one mode to the other. Therefore, during a trial, each electrode can be used either for stimulation or recording. Voltage stimulation consisted of bipolar pulses lasting 100 μs at each polarity, of amplitude varying from 0.2 V to 1 V, injected through the STG1004 Stimulus Generator. An artifact lasting 5 – 20 ms caused by the electrical stimulation was induced on the recording electrodes but was removed from the electrical recordings during data analysis.

Tetanus: The tetanus, i.e., a high frequency stimulation, consisted of 40 trains of bipolar pulses of $+/- 0.9$ V lasting for 200 μs delivered every 2 s. Every train consisted of 100 pulses at 250 Hz. Test stimuli before and after tetanus were delivered every 2 s. The tetanus had a spatial profile usually composed by two perpendicular bars of electrodes meeting in a corner, or by a vertical or horizontal bar of electrodes.

G. Data Analysis

Acquired data were analyzed using the software MatLab (The Mathworks, Inc., Natick, MA).

Artifact Removal: The artifact at each electrode and for each pattern of stimulation was estimated and subtracted from the voltage recordings. The artifact was estimated in the following way: for each pattern of stimulation and at each electrode the voltage response was averaged over all trials (typically 50), computed and fitted by 2 polynomials of ninth degree. Using polynomials of a lower order provide similar results in most of experiments, but not in all, therefore, ninth degree polynomials were routinely used. The 2 polynomials fitted respectively the data in the time windows of 0.5–25 ms and 7.5–100 ms after stimulation. The first polynomial was used to evaluate the artifact in the time window of 0.5 to 7.5 ms, while the second in the time window of 7.5 and 82.5 ms. The artifact, so evaluated, was subtracted from the original voltage signal. The time window between 0 and 1 ms after stimulation was not considered in the data analysis.

Computation of Firing Rate ($\text{FR}_{ij}(t)$) and Related Quantities ($\text{AFR}_{ij}(t)$, $\text{FR}(t)$, $\text{AFR}(t)$, IntAFR_{ij} , IntAFR , IntFR): Let $V_{ij}(t)$ be the voltage recorded at electrode (i, j) and σ_{ij} be the standard deviation of the noise computed considering a period of at least 1 s where no spikes were visually observed. The σ_{ij} of the noise ranged for individual electrodes from 3 to 6 μV . Action potentials are considered to be events exceeding 5 σ_{ij} . The firing rate per electrode $\text{FR}_{ij}(t)$ is computed with a binwidth of 10 ms centered on t. The $\text{FR}_{ij}(t)$ counts spikes from different neurons, making a good electrical contact with electrode (i, j). The average firing rate $\text{AFR}_{ij}(t)$ was computed by averaging $\text{FR}_{ij}(t)$ over the entire set or a subset of identical stimulations [Figs. 1(e), (f) and 5(a), (b)]. Let active electrodes be the electrodes showing a clear electrical contact with the neuronal culture, i.e., where spikes can be recorded. Generally, in order to have a simple measure of the overall evoked firing rate, the firing rate spatially averaged $\text{FR}(t)$ was obtained by averaging $\text{FR}_{ij}(t)$ over the entire set of active recording electrodes. Only for the computation, shown in Figs. 2(a) and 3(a), the spatial average was limited to a row of electrodes. The average overall

TABLE I

Abbreviations / Names of variables	Definitions	Figure
$FR_{ij}(t)$ Firing rate	Firing rate per electrode in either 5 or 10 ms bins with centers specified by t	
$AFR_{ij}(t)$ Average firing rate	Firing rate per electrode averaged over the entire set or a subset of identical stimulations	1E, 1F, 5A, 5B
$\overline{FR}(t)$ Firing rate spatially averaged	Firing rate spatially averaged over a set of recording electrodes	
$\overline{AFR}(t)$ Average overall evoked response	Average of $\overline{FR}(t)$ over the entire set or a subset of identical stimulations	3B, 4C, 5C, 5D
$\text{Int}AFR_{ij}$	Integral between $t=1$ ms and $t=50$ ms of $AFR_{ij}(t)$	4A
$\text{Int}\overline{AFR}$	Integral between $t=1$ ms and $t=50$ ms of $\overline{AFR}(t)$	7
$\text{Int}\overline{FR}$	Integral between $t=1$ ms and $t=50$ ms of $\overline{FR}(t)$	6

evoked response $\overline{AFR}(t)$ is the average of $\overline{FR}(t)$ over the entire set or a subset of identical stimulations [Figs. 3(b), 4(c), and 5(c), (d)]. The coefficient of variation $CV(t)$ of $AFR_{ij}(t)$ was computed as the ratio of the standard deviation of $FR_{ij}(t)$ to the $AFR_{ij}(t)$. Similarly, the coefficient of variation $CV(t)$ of $\overline{AFR}(t)$ was computed as the ratio of the standard deviation of $\overline{FR}(t)$ to the $\overline{AFR}(t)$. In order to describe the properties of the neuronal culture to learn and discriminate patterns, the integrals respectively of $AFR_{ij}(t)$, $\overline{FR}(t)$, $\overline{AFR}(t)$ in a time window between 1 and 50 ms have been calculated and defined as, $\text{Int}AFR_{ij}$, $\text{Int}\overline{FR}$, $\text{Int}\overline{AFR}$. $\text{Int}AFR_{ij}$ and $\text{Int}\overline{AFR}$ were used to compare the average response evoked by an identical stimulation before and after the tetanization, at a single electrode and when all the MEA electrodes were considered [see Figs. 4(a), 7, respectively]. $\text{Int}\overline{FR}$ was used to compare at the level of a single-trial the response evoked by different patterns of stimulation, detected by all the MEA electrodes (see Fig. 6). The different quantities used to characterize the firing of the neuronal culture are reported in Table I.

H. Pattern of Stimulation and Image Processing

The input to the device is the set of extracellular voltage stimulations, delivered at time $t = 0$, applied to the neuronal culture through the MEA electrodes. If (i, j) is an electrode of the MEA, the input is the matrix S_{ij} of voltage stimulations applied to the electrode (i, j) . A binary image or pattern I_{ij} of $M \times N$ pixels [Fig. 1(a)] is coded into the input of a MEA with $M \times N$ electrodes [Fig. 1(b)], so that the gray level of pixel (i, j) of I_{ij} is converted into the appropriate voltage stimulation S_{ij} of electrode (i, j) . The matrix of voltage signals $V_{ij}(t)$ recorded with the MEA [Fig. 1(c)], composed of action potentials or spikes produced by the neurons in the culture [Fig. 1(b)] is analyzed. The output of the device is the matrix $FR_{ij}(t)$. MEAs with at least 54 electrodes providing electrical recordings of clear spikes were used for image processing. For each pattern of electrodes used for stimulation, let $S_{1/2}$ be the voltage stimulation evoking half of the maximal $\overline{AFR}(t)$ in the time window between 1 and 11 ms after the onset of the voltage pulse. If I_{ij} is the corresponding binary image or the pattern to be processed and its gray levels are either 0 or 1, then S_{ij} will be $3/2 * S_{1/2}$ if I_{ij} is 1, 0 otherwise.

Filling Silent Electrodes and Smoothing: The procedure here described has been applied only for image processing [Figs. 2(b), (c), 3(d), and 8]. MEAs with at least 54 electrodes

providing electrical recordings of clear spikes were used. When one electrode (i, j) is silent, i.e., no spikes can be recorded, the corresponding hole in the processed image is filled in by assigning to $FR_{ij}(t)$ the value obtained by averaging the firing rate from neighboring electrodes – i.e., electrodes at a distance of $500 \mu\text{m}$. $FR_{ij}(t)$ of stimulated electrodes was determined by extrapolation from the neighboring active electrodes using (1). All processed images had at most 3 silent electrodes, including the one used as ground. The value of $FR_{ij}(t)$ was smoothed over the neighboring electrodes $(i - 1, j)$, $(i + 1, j)$, $(i, j - 1)$ and $(i, j + 1)$.

Processing of 8 Bit Images: The 8-bit image O_{ij} was described by

$$\sum_{p=1}^8 I_{ij}^{(p)} 2^{(p-1)}$$

where $I_{ij}^{(p)}$ is a 1-bit image. The 8 $I_{ij}^{(p)}$ 1-bit images are processed as described below and their output was summed as described in (4) and (5).

Scaling of $FR_{ij}(t)$, $AFR_{ij}(t)$ and Output Color-Coding: In order to display processed images using a standard color-coding, the values of $FR_{ij}(t)$, $AFR_{ij}(t)$ or their combination (for bandpass filtering) were rescaled. The scaling procedures described in this section refer to the factors α and $\alpha^{(p)}$ of (2), (4) and (5) (see Results). For low-pass filtered images, the values of $FR_{ij}(t)$ [Fig. 3(d)] or $AFR_{ij}(t)$ [Fig. 2(b), upper row] were scaled between 0 and 1 by dividing for the corresponding maximal value among all electrodes in the time-window 1–30 ms. Digitally low-pass filtered images [Fig. 2(b) lower row] were scaled between 0 and 1 dividing by their maximal value. Bandpass filtered image [Fig. 2(c) top panel] was obtained as the difference of $AFR_{ij}(t)$ calculated in time bins 1–6 ms and 4–9 ms and the resulting matrix was scaled between -1 and $+1$, dividing by its maximum absolute value. For digitally bandpass filtered images [Fig. 2(c) lower panel], obtained as the difference of digitally low-pass filtered images, the resulting output was scaled between -1 and $+1$, dividing for its maximum absolute value. The color map (of 256 colors) was always scaled between -1 and 1 . For 8-bit processed images [Fig. 8(a)], the values of $AFR_{ij}(t)$ were scaled as described above, and were added according to (4). When it was necessary to compare 8-bit image processing before and after tetanization [see Fig. 8(b)], the values of $AFR_{ij}(t)$ obtained

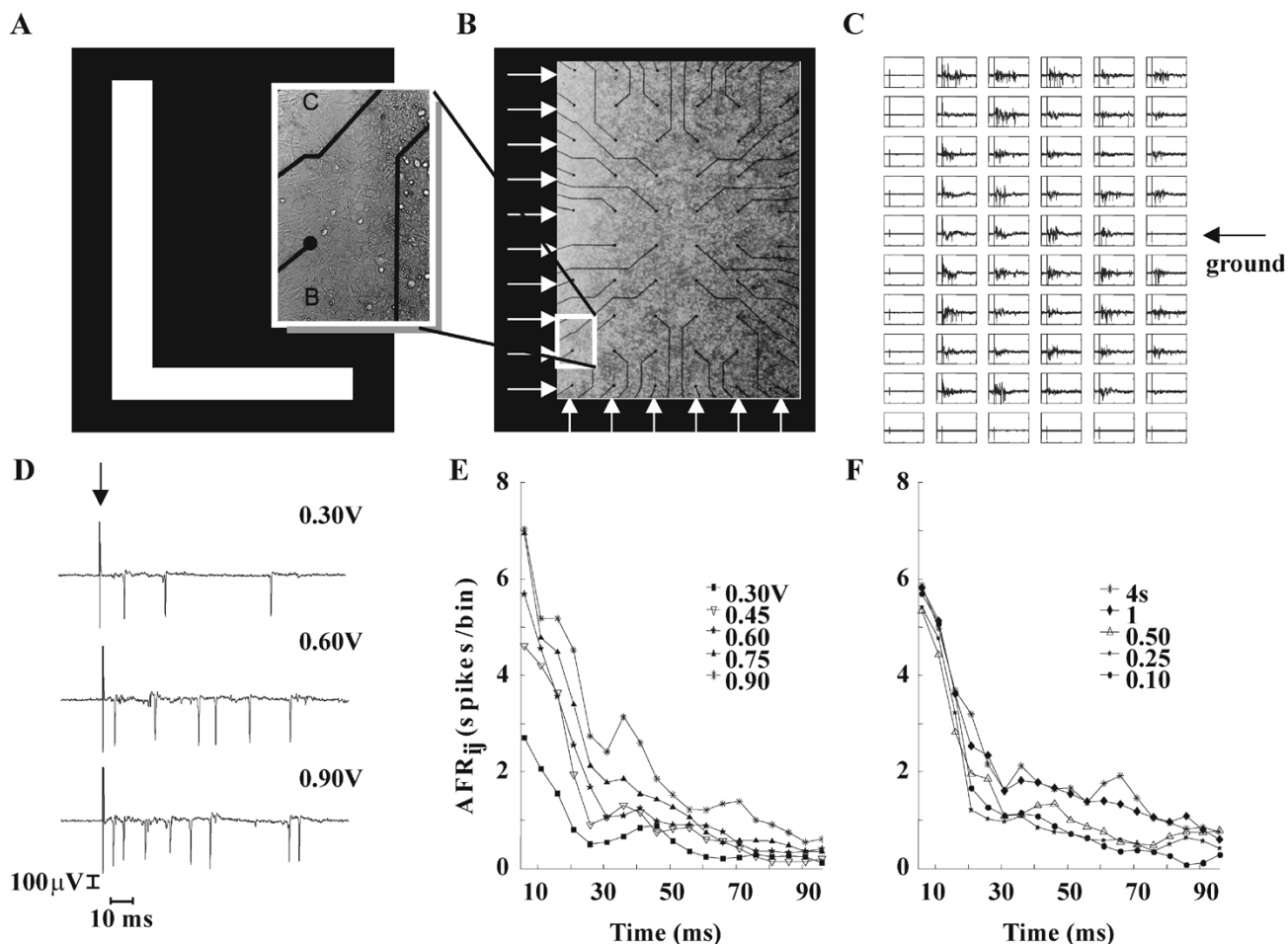


Fig. 1. Mapping an image into the stimulation of a neuronal culture. (A) 10×6 binary image of a 1 used as the stimulation pattern of a neuronal culture grown over a 10×6 MEA manufactured by MCS. (B) Photo of dissociated hippocampal neurons grown on the MEA. Magnification of the neuronal culture on the area marked by the letters B and C (white rectangle) shown in the inset. (C) Electrical recordings of electrical activity evoked by the electrodes stimulation with bipolar voltage pulses of 0.9 V. The silent electrode indicated by the arrow was used as the ground. (D) Three voltage recordings evoked by voltage pulses of 0.3, 0.6, and 0.9 V when the 6 electrodes of the upper row were stimulated. (E) $AFR_{ij}(t)$ (see Section II) recorded by a representative electrode in response to five different voltage stimulations, as indicated in the panel. (F) $AFR_{ij}(t)$ recorded by a representative electrode at different repetition rates as indicated in the panel. Data in (E) and (F) are averaged from 50 different trials of the same stimulation. Time 0 ms corresponds to the voltage stimulation.

after tetanization were scaled dividing by the maximal value of $AFR_{ij}(t)$ measured before tetanization. In this case the scaled values of $AFR_{ij}(t)$ before tetanization varied between 0 and 1, but, after tetanization, they could be larger than 1. The scaled values of $AFR_{ij}(t)$ were added according to (5). The color map (of 256 colors) was scaled between 0 and 256. Therefore, with this coding, the processing of images at 1 or 8-bit has the same map, i.e., the output has 256 different colors.

III. RESULTS

A. The Device

The great majority of MEAs presently available and charge-coupled device (CCD) arrays share the same geometry of a square grid. Therefore, CCD pixels and MEA electrodes can be put in a simple one-to-one correspondence preserving their neighborhood [see Fig. 1]. This observation inspired the design of a new device for processing images and patterns, using a MEA and a neuronal culture grown on its surface. The image is mapped to the voltage stimulation of the neuronal culture and

the evoked electrical activity is taken as the output of the device. The computing elements of the device are the neurons of the culture.

The input to the device is the set of extracellular voltage stimulations, delivered at time $t = 0$, applied to the neuronal culture through the MEA electrodes, coding for the image I_{ij} to be processed. The output of the device is the matrix $FR_{ij}(t)$, counting the number of times in which the extracellular voltage recorded at electrode (i, j) exceeds a given threshold in the time window between $t - \Delta t$ and $t + \Delta t$. Several average quantities – in space, time and over different trials – were computed from $FR_{ij}(t)$ (see Section II for further details).

B. Dynamic Range and Cycle Time

In order to explore the dynamic range and cycle time of the proposed device, a row of electrodes, was repeatedly used for stimulation. Brief ($200 \mu s$) bipolar voltages with amplitude varying from 0.3 V to 0.9 V were used. When the voltage stimulation was increased, the frequency of evoked spikes increased and often spikes with a novel shape, produced by a different neuron, appeared [Fig. 1(d)]. The average firing

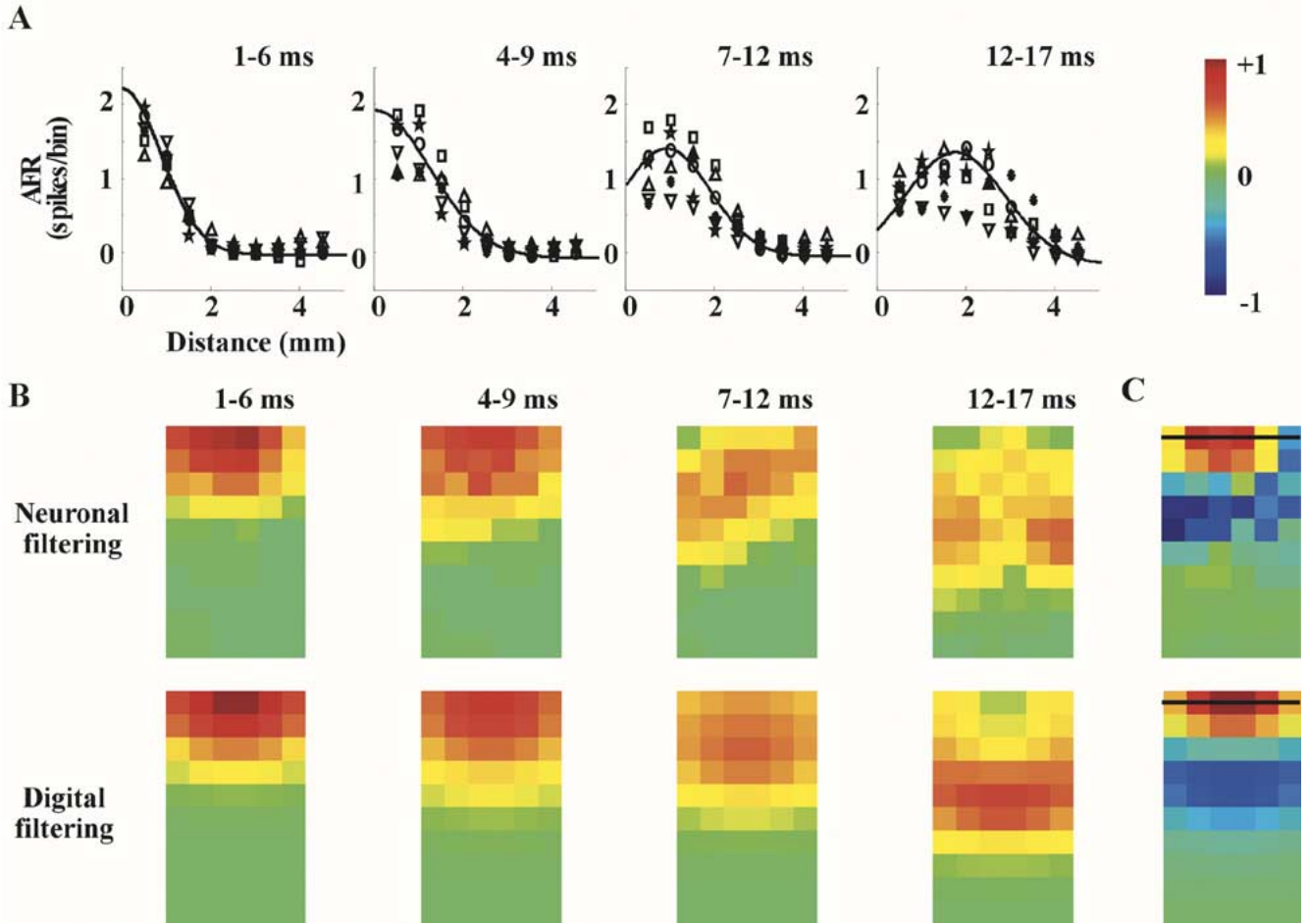


Fig. 2. Spread of excitation through the neuronal culture. (A) $\overline{AFR}_{ij}(t)$ averaged by row ($\overline{AFR}(t)$) and calculated in the time windows of 1–6, 4–9, 7–12 and 12–17 ms after the stimulation of the uppermost row of electrodes with a voltage pulse of 0.6 V. Different symbols indicate experimental data from 6 different neuronal cultures. Thick curves are theoretical fits calculated from (1). Data obtained in the time windows 1–6 and 4–9 ms were fitted by setting $\tilde{\rho}$ equal to 0 and σ respectively, to 890 and 1240 μm . Data in the time windows 7–12 and 12–17 ms were obtained with $\tilde{\rho}$ equal to 920 and 1750 and σ equal to 980 and 1130 μm respectively. (B) Comparison between neuronal and digital filtering. (Upper row) images obtained from the processing performed by the neuronal culture in the corresponding time windows. (Lower row) digital Gaussian filtering of the original binary image with the uppermost row of pixels equal to 1 and 0 elsewhere. (C) (Upper panel) bandpass filtering of the neuronal culture obtained by subtracting the AFRs in the time windows 1–6 and 4–9 ms; (lower panel) digital filtering obtained by convolving the original binary image with the difference of two Gaussians fitting the experimental data in the first and second panel of Fig. 2(a). The thin bars indicate the stimulated electrodes. Color-coding is reproduced at the right side of panel A.

$\overline{AFR}_{ij}(t)$ increased with the voltage stimulation [Fig. 1(e)], but its dynamic range was rather narrow: usually no spikes were evoked by voltage pulses below 0.2 V and a saturating maximal response was evoked with voltage stimulation of about 1 V. In the vast majority of the experiments, it was possible to distinguish reliably 4 levels of evoked activity.

In order to determine the cycle time of the device, the same stimulation was repeated at intervals from 0.1 s to 10 s. With a repetition interval higher than 1 or 2 s the $\overline{AFR}_{ij}(t)$ had two components: one which was evoked with a delay of very few ms and lasting for about 15 ms, followed by a second lasting around 0.1 s. The amplitude of the first component was not significantly affected by decreasing the repetition time from 4 to 0.1 s [see Fig. 1(f)]. The amplitude of the second component was clearly depressed at short repetition times and it was stable for repetition times greater than 4 s (data not shown).

C. Filtering Properties of the Neuronal Culture

The neuronal culture grown on the MEA constitutes a two-dimensional (2-D) network. Given a homogenous culture, its fil-

tering properties can be simply analyzed by using a long bar as a spatial stimulus, thus reducing a 2-D problem to a much simpler one-dimensional. In these experiments the six electrodes of the upper row were used for stimulation and the average firing rate evoked in each electrode was measured (see Section II) and averaged by row ($\overline{AFR}(t)$). At early times, i.e., in the time window between 1 and 6 ms [Fig. 2(a)] the $\overline{AFR}(t)$ decayed as a Gaussian function with a standard deviation σ of about 900 μm corresponding to 1.8 pixels (solid line). In the time window between 4 and 9 ms the electrical activity decayed similarly as a Gaussian function but with a larger σ of about 1200 μm corresponding to 2.5 pixels (solid line). A very similar decay and spread of electrical excitation was consistently observed in all the 24 analyzed neuronal cultures. Data collected from 6 different dishes are shown in Fig. 2 as different symbols.

After about 10 ms from the stimulus, the peak of the $\overline{AFR}(t)$ moved away from the stimulated electrodes and the spread of the electrical activity could be described by a Gaussian function centered at a distance $\tilde{\rho}$ from the stimulated electrodes [Fig. 2(a), time interval of 7–12 ms]. After 15 ms the evoked electrical ac-

tivity decayed even further, maintaining a Gaussian-like profile [Fig. 2(a), time interval of 12–17 ms]. While the same qualitative behavior was observed in all neuronal cultures, after at least 25 days of cultivation, the speed at which the electrical activity moved from the stimulating electrodes varied between 70 to 250 $\mu\text{m}/\text{ms}$. The electrical activity in young cultures, i.e., with less than 20 days, did not propagate well throughout the culture.

A comparison between the spatio-temporal filtering performed by the neuronal culture and a digital gaussian filtering is shown in Fig. 2(b). The processing of the bar-stimulus by the neuronal culture represented by the color-coding of the evoked $\text{AFR}_{ij}(t)$ is shown in the upper row of Fig. 2(b) in the four time windows. The corresponding digital convolution of the binary image correspondent to the bar-stimulus (see Section II) is shown in the lower panels of Fig. 2(b). Between 1 and 9 ms the neuronal filtering is a good approximation of a Gaussian digital filtering which used the σ extracted from the fit of Fig. 2(a). Between 7 and 12 ms (and 12–17 ms), the Gaussian filtering with the values of $\tilde{\rho} = 1250 \mu\text{m}$ and $\sigma = 850 \mu\text{m}$ (and $\tilde{\rho} = 1750 \mu\text{m}$ and $\sigma = 1130 \mu\text{m}$) shows the same features of the neuronal filtering. Therefore, at later times, $\text{AFR}_{ij}(t)$ is a noisy displaced low-pass filtering of the original image.

When an horizontal bar in a different location or a vertical bar of electrodes was used to stimulate the neuronal culture, the electrical activity propagated from the stimulation site with almost the same properties of the horizontal bar in the upper part shown in Fig. 2(a) and (b). Experiments where a row (or a column) of electrodes or individual electrodes were stimulated indicate that the spatial-temporal processing of the neuronal culture is – to a first approximation – spatially invariant and can be described by a radial impulse response with a Gaussian function or kernel, centered on $\tilde{\rho}$ and with a time varying variance $\sigma^2(t)$

$$h(\rho, t) = \exp\left(-\frac{(\rho - \tilde{\rho}(t))^2}{2\sigma^2(t)}\right) \quad (1)$$

and ρ is the polar coordinate of the electrode.

Therefore, given a 1-bit image I_{ij} the output of the proposed device $\text{FR}_{ij}(t)$ varies in time according to

$$\text{FR}_{ij}(t) = \alpha \cdot I_{ij} ** h(\rho, t). \quad (2)$$

** indicates a 2-D convolution and α is a scaling factor (see Section II). As shown in Fig. 2(b), in the time window 1–6 ms, the impulse response of the neuronal culture is a Gaussian function with a σ of about 900 μm , but 2 or 3 ms later with a larger value of σ of about 1200 μm . The neuronal filters obtained in the time windows 1–6 ms and 4–9 ms are low pass, and their difference is bandpass (see Section II). Bandpass filtering of the binary image corresponding to the bar-stimulus obtained with the neuronal culture, is shown in the upper panel panels of Fig. 2(c). This neuronal filtering is rather similar to that obtained by a digital band-pass filtering, shown in the lower panel of Fig. 2(c) (see Section II).

D. Reproducibility of Neuronal Firing and Filtering

Unlike silicon devices, biological neurons are affected by a significant noise and their reliability is variable. In our neuronal cultures, during repetitions of the same stimulations, the number

of evoked spikes measured by a single electrode was variable, but often the first evoked spike was rather reliable with a jitter varying from just a few hundreds μs to some ms.

The reproducibility of neuronal firing measured by a single electrode was evaluated computing the coefficient of variation $\text{CV}(t)$ of $\text{AFR}_{ij}(t)$ (see Section II). When the value of CV is less than 0.4, the firing is considered reproducible. Fig. 3(a) shows the $\text{CV}(t)$ of the evoked response recorded by the electrodes in the 2nd (left panel, open symbols) and in the 7th (right panel, open symbols) rows of the array [Fig. 3(c)]. For the electrodes in the 2nd row, in the time window between 1 and 11 ms, the $\text{CV}(t)$ was for most electrodes smaller than 0.5 and could approach 0.2. For the electrodes in the 7th row, in the time window between 11 and 16 ms, the $\text{CV}(t)$ was always smaller than 0.75 and could approach 0.3. The value of the $\text{CV}(t)$ was slightly higher at increasing distances of the recording electrode from the stimulation site. These results indicate that there is a “reliability window” soon after the stimulation in which the $\text{CV}(t)$ of the evoked activity at most electrodes is less than 0.5 and often around 0.3.

The $\text{CV}(t)$ of the evoked response was further decreased by considering all the spikes recorded from a row of electrodes, as shown in Fig. 3(a) (thick line). The $\text{CV}(t)$ was between 0.1 and 0.2 for both the electrode rows and the $\text{CV}(t)$ remains less than 0.5 for at least 20 ms. When all the spikes recorded from all electrodes on the MEA were pooled together, the $\text{CV}(t)$ of the evoked response was transiently lower than 0.1 (in the time window between 11 and 21 ms) and remained less than 0.3 for at least 45 ms [see Fig. 3(b)]. Therefore, considering larger pools of neurons, the reliability of the response is improved and extended to larger time windows.

Fig. 3(d) illustrates images obtained from three single trials when the uppermost row of electrodes was stimulated with the same voltage pulse of 0.6 V. While at early times, during the so called “reliability window,” the spread of the evoked activity in different trials was rather similar, at later times, the spread differed from trial to trial consistently with the high $\text{CV}(t)$ of the electrical recordings [see Fig. 3(a)]. Neuronal cultures obtained from different rats and cultivated in different dishes had a variable number of active electrodes, i.e., providing good electrical recordings, ranging from 30 to 58. All neuronal cultures, with a sufficient number of electrically active electrodes to allow a quantitative characterization of the filtering of the neuronal network, i.e., larger than 40, had the same behavior illustrated in Fig. 2(a). A very similar decay and spread of electrical excitation was consistently observed in all the analyzed neuronal cultures. At early times the spread of electrical excitation was characterized by a Gaussian function with a standard deviation increasing from 800 to 1200 μm in about 3 ms. At later times the behavior of different neuronal cultures [Fig. 2(a)] was more variable than the response of an individual culture [see Fig. 3(a)]. These data show that immediately after the voltage stimulation there is a “good” time window during which the processing of the neuronal culture is reproducible leading to a reliable computation. This reproducibility is observed among trials from the same neuronal culture [see Fig. 3] and in different cultures [see Fig. 2(a)]. Since neuronal cultures could be maintained up to six months, it was possible to repeat several times the same experiment in the same culture and to verify that the spread of electrical excitation in the same culture had identical properties

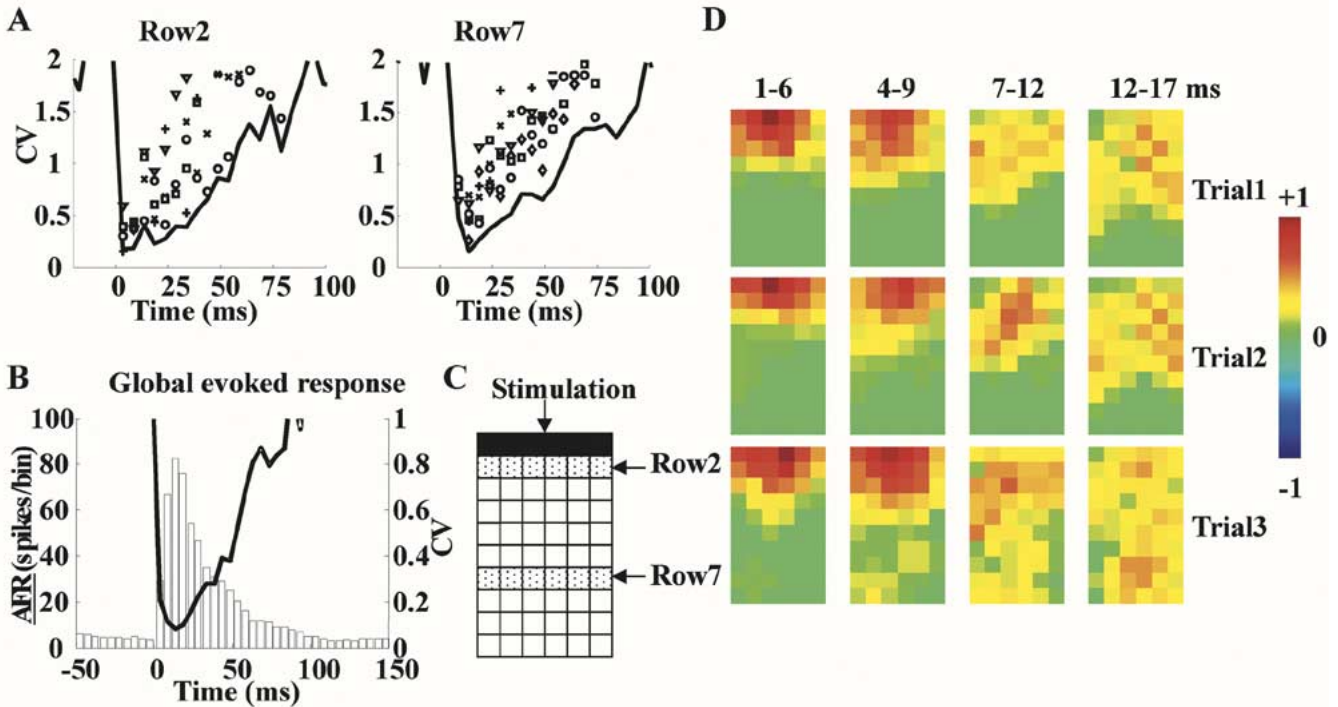


Fig. 3. Reproducibility of the neuronal firing and reproducibility of the spread of the excitation. Data obtained stimulating the uppermost row of electrodes (shown as black squares in panel C). (A) $CV(t)$ of the evoked response considering the spikes recorded from each single electrode (open symbols) and from the row of electrodes (thick line), in the second (left panel) and the seventh (right panel) rows of the array. (B) $\overline{AFR}(t)$ and $CV(t)$ of the spikes recorded from the entire array of active recording electrodes (excluding the 1st row used for stimulation). (C) Map of the MEA electrodes analyzed in (A) and (B). (D) Spread of the excitation in different trials of stimulation. Each row reproduces images obtained from a single sweep or trial, in the four time windows after stimulation indicated at the top of each column. The $FR_{ij}(t)$ in each image is represented according to the color map reproduced at the right side of the figure.

when analyzed in different days (in a time window of approximately two weeks).

E. Learning

Having characterized the filtering properties of the neuronal cultures, we investigated whether it was possible to induce learning in the neuronal culture [20]–[23] in a consistent and controlled way. If so, is it possible to train the neuronal culture to recognize a specific spatial pattern?

Learning in neurons is associated with changes in synaptic efficacy, leading to a persistent increase in amplitude of the response to the “learnt” stimulus. This is usually referred to long-term potentiation (LTP) and can be induced by delivering a tetanus (usually trains of stimuli at 100 Hz or more) to the neuronal culture. We refer to a \lceil -stimulus (\lceil -stimulus) when the stimulation was applied to two perpendicular bars of electrodes forming an \lceil and to a \lceil -tetanus when the tetanus had the same spatial profile of the \lceil -stimulus.

To test the ability of hippocampal cultures to learn, the electrical response to a \lceil -stimulus before and after the application of a \lceil -tetanus was compared. The \lceil -stimulus was delivered to the neuronal culture every 2 s. The evoked electrical activity was monitored by computing $\text{Int}AFR_{ij}$ (see Section II). After the \lceil -tetanus, the $\text{Int}AFR_{ij}$ [Fig. 4(a)] and the electrical activity in individual traces [Fig. 4(b)] evoked by the \lceil -stimulus were significantly increased for at least 1 hour.

The firing rate averaged over different trials and over all MEA electrodes, $\overline{AFR}(t)$, is a global indicator of the changes induced by LTP. The $\overline{AFR}(t)$ evoked by the \lceil -stimulus clearly

increased after \lceil -tetanus in the time window between 10 and 90 ms after the stimulation. Fig. 4(c) shows the averaged data from 4 neuronal cultures before (left panel) and after (right panel) \lceil -tetanus.

As LTP can be induced in the neuronal cultures, it is necessary to establish its spatial structure. Therefore, the electrical activity evoked by stimuli with different spatial profiles was compared. Neuronal cultures were stimulated every 2 s with \lceil -stimulus and \lceil -stimulus. Prior to \lceil -tetanus, the \lceil -stimulus and the \lceil -stimulus evoked a similarly diffused response [see $\overline{AFR}_{ij}(t)$ in left and right panel of Fig. 5(a)]. This was also evident when the firing rate was averaged over different trials and over all recording electrodes ($\overline{AFR}(t)$) [see left and right panels in Fig. 5(c)]. After the \lceil -tetanus, only the response to the \lceil -stimulus significantly increased [Fig. 5(b)] being more than twice the response evoked by the \lceil -stimulus [compare left and right panels in Fig. 5(d)].

In Figs. 4 and 5, learning and pattern discrimination was examined by averaging responses over different trials. A useful device, however, must be able to discriminate between patterns on the basis of a single trial, and its learning capabilities should be evident by inspection of a single trial. The single response was evaluated computing $\text{Int}FR$ (see Section II). Fig. 6(a) shows single-trial responses for a \lceil -stimulus (open symbols) and a \lceil -stimulus (filled symbols). Prior the application of the \lceil -tetanus, single-trial responses to the two stimuli could not be distinguished reliably. After \lceil -tetanus the single-trial response to the \lceil -stimulus was consistently larger than the single-trial response evoked by the \lceil -stimulus.

Fig. 6(b) reproduces the distribution of single-trial responses for the \lceil -stimulus (white bars) and the \lceil -stimulus (black

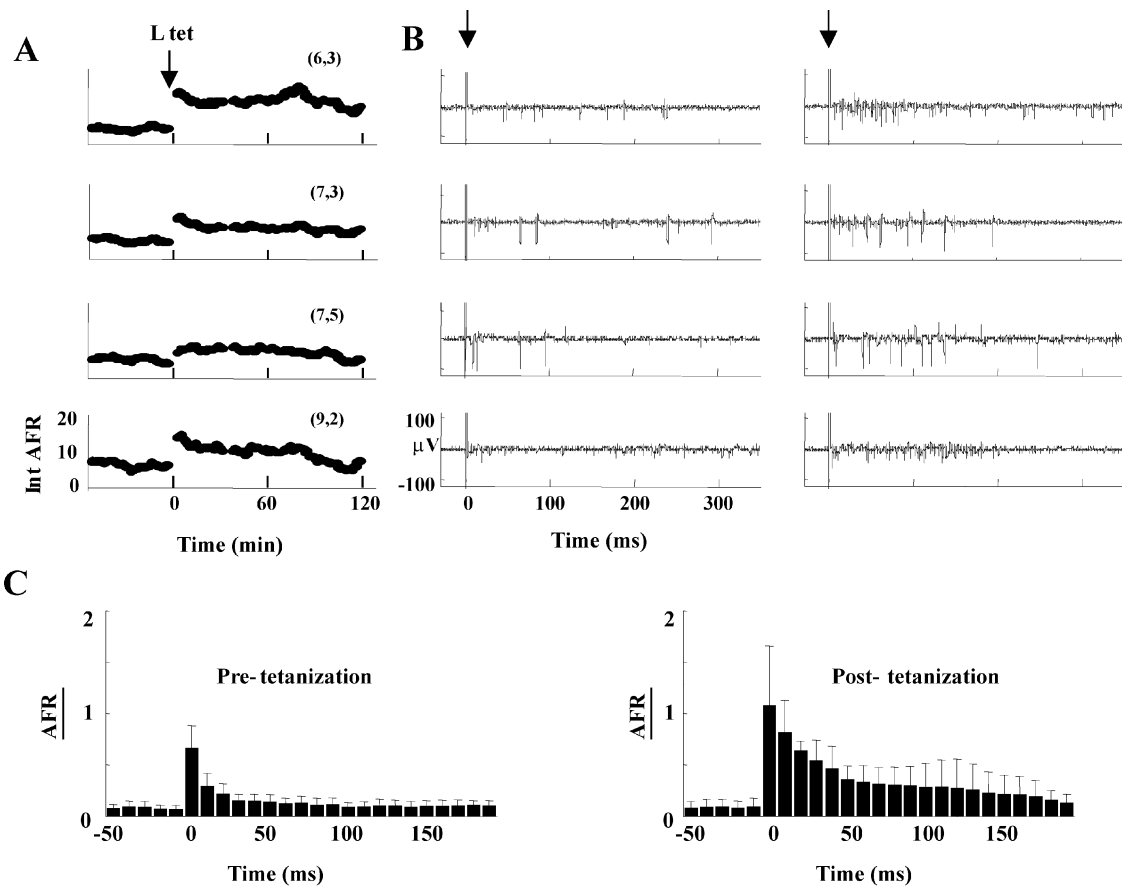


Fig. 4. Induction of LTP in a neuronal culture from hippocampal neurons. (A) Time-dependence of IntAFR_{ij} prior to and after \lfloor -tetanus for the electrodes (6,3), (7,3), (7,5), and (9,2), with tetanus indicated by an arrow. Each point was obtained by averaging 20 responses to the same stimulation repeated every 2 s. \lfloor -tetanus was performed as described in Section II. (B) Single extracellular voltage response obtained before (left) and after tetanization (right) from the electrodes shown in A. Time zero, indicated by the arrow, corresponds to the delivery of the stimulation. The large transient at time zero is the residual artifact after its subtraction (see Section II). (C) $\underline{\text{AFR}}(t)$ and standard deviation of an \lfloor -stimulus calculated averaging 4 different experiments before and after the \lfloor -tetanus. $\underline{\text{AFR}}(t)$ was obtained averaging single sweeps measured in a time window of 30 min.

bars) before (left panel) and after (right panel) \lfloor -tetanus. The experimental distributions were fitted with Gaussian functions of unitary area and the superimposed area of the two curves was calculated. Before \lfloor -tetanus the average value of the single-trial responses for the \lfloor - and the \lceil -stimulus was 4.7 ± 0.8 and 5.6 ± 0.8 respectively. In 58% of cases the presented stimulus could not be recognized on the basis of the single-trial response (superimposed area). After tetanus the average value of single-trial responses for the \lfloor and \lceil -stimuli was 4.1 ± 0.5 and 6.4 ± 0.7 respectively. Now, the superimposed area of the two Gaussian functions fitting the experimental distributions was reduced to 5.5%. As a consequence, after tetanus, it was possible to recognize the presented stimulus from its single-trial response with an accuracy of about 94.5%.

Results of similar experiments from 4 neuronal cultures are presented in Fig. 6(c). The distribution of single-trial responses (IntFR) before (left panels) and after (right panels) \lfloor -tetanus for the \lfloor and \lceil -stimulus are shown as black and white bars respectively. Before \lfloor -tetanus, the distributions of the IntFR for the 2 patterns were almost completely overlapping. After \lfloor -tetanus in all 4 neuronal cultures, single-trial responses were modified so that it was possible to discriminate the stimulating pattern

from the great majority of single-trial responses. In fact, after tetanus, single-trial responses for the two stimuli were distinguishable for 80%, 98%, 78% and 95% in the 4 neuronal cultures. In general, when the tetanus was applied to two perpendicular bars of electrodes meeting in a corner, the response to the stimulation applied to the same bars of electrodes increased, while the response to the stimulation applied to distinct perpendicular bars of electrodes meeting in the opposite corner was never potentiated.

If the neuronal culture can be trained to discriminate between a \lfloor -stimulus and a \lceil -stimulus it is important to analyze the selectivity of this recognition and verify whether it degrades “gracefully” with the corruption of the stimulus. Therefore, the evoked responses to stimuli with different spatial profiles prior to and after \lfloor -tetanus were compared.

Prior to \lfloor -tetanus, the response of the neuronal culture was not specific to the spatial profile of the stimulus [Fig. 7(a) open circles]. On the contrary, after \lfloor -tetanus, the neuronal culture preferentially responded to stimuli resembling to an \lfloor [Fig. 7(a) filled circles]: in fact, after \lfloor -tetanus, the IntAFR was significantly larger for stimuli with a spatial profile similar to \lfloor (for the five stimuli from the left of the x-axis, t-test $p < 0.001$). The relative change of the IntAFR after \lfloor -tetanus was clearly

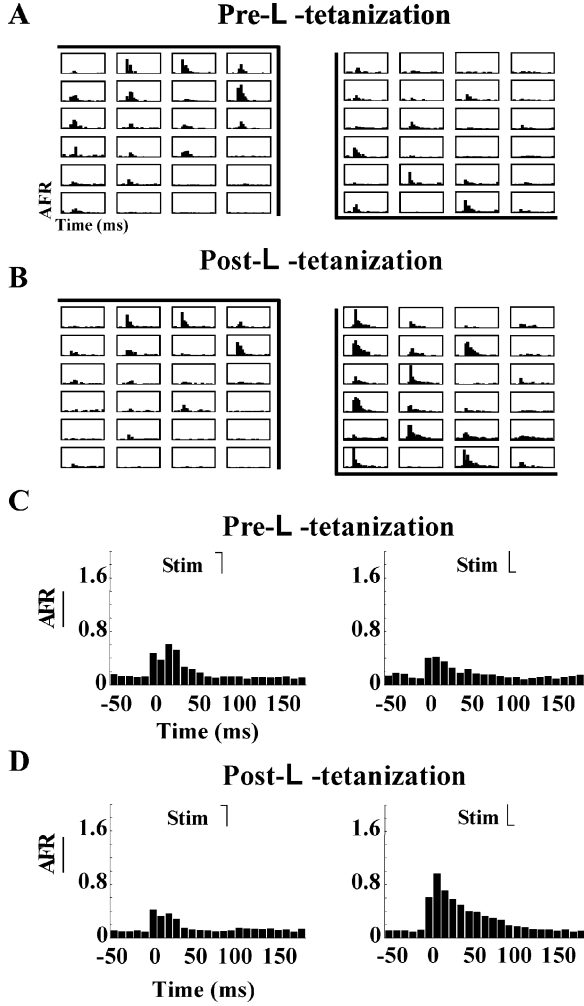


Fig. 5. Neuronal cultures can learn to distinguish between two different spatial profiles. (A) $AFR_{ij}(t)$ evoked by the]-stimulus (left) and the [-stimulus (right) recorded from 24 electrodes (Y-axis limits: 0 to 10 spikes/bin; X-axis limits: -50 to 200 ms). During the experiment the]-stimulus and a [-stimulus were alternated every 2 s. $AFR_{ij}(t)$ in (A) were obtained averaging the individual responses recorded in a time window of 30 min before tetanus. (B) As in (A) but in the time window of 30 min after the]-tetanus. (C) $\overline{AFR}(t)$ obtained by averaging the $AFR_{ij}(t)$ over all the active recording electrodes. The 2 $\overline{AFR}(t)$ shown refer to the responses to the]-stimulus (left) and the [-stimulus (right) before]-tetanus. (D) $\overline{AFR}(t)$ obtained by averaging the $AFR_{ij}(t)$ over all the active recording electrodes. The 2 $\overline{AFR}(t)$ shown refer to the responses to the]-stimulus (left) and the [-stimulus (right) after]-tetanus.

selective [Fig. 7(b)] and showed positive value for similar spatial profiles.

F. Image Processing of 8-Bit Images and Feature Extraction

The neuronal culture can be used also for processing digital images at 8 bits. Let O_{ij} be an image with 8 bit gray levels at location (i, j) . Then O_{ij} can be represented by the decomposition

$$O_{ij} = \sum_{p=1}^8 I_{ij}^{(p)} 2^{(p-1)} \quad (3)$$

where $I_{ij}^{(p)}$ is a 1-bit image.

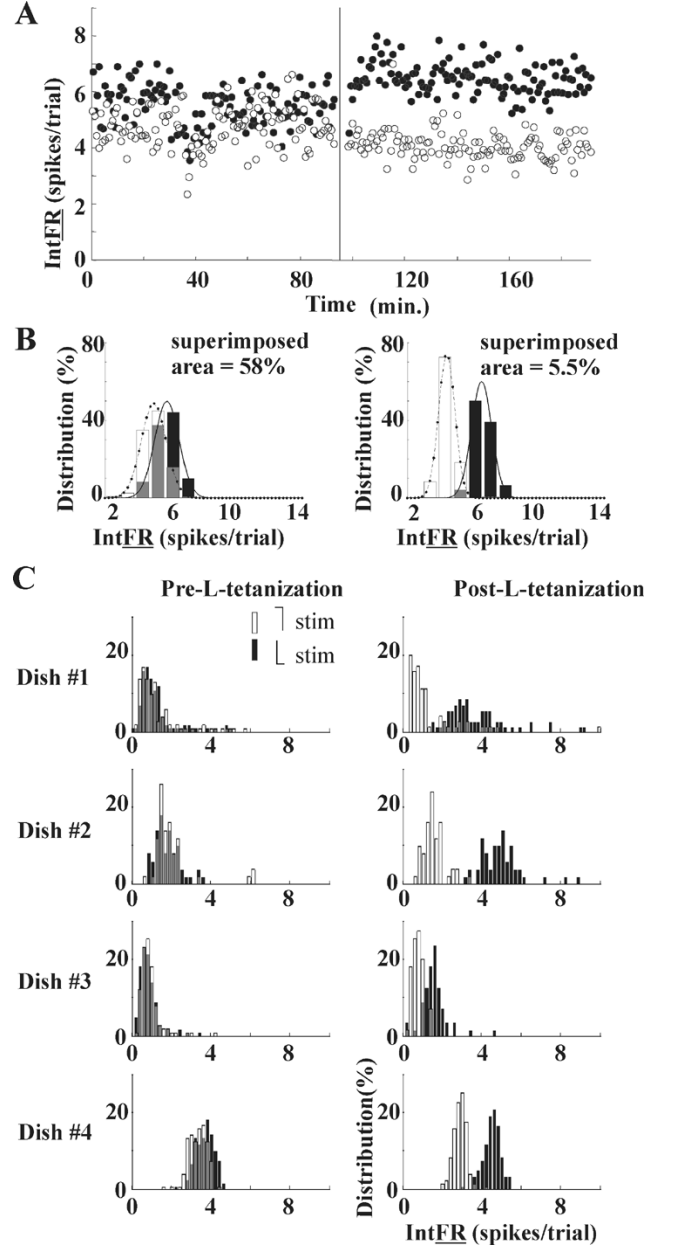


Fig. 6. Discrimination at single-trial level before and after]-tetanus for a neuronal culture.]-stimulus and [-stimulus have been analyzed. (A) Time-evolution of the IntFR evoked by a]-stimulus (open symbols) and an [-stimulus (black symbols) prior and after a]-tetanus (indicated by a black vertical line). (B) Distribution of the IntFR before (left panel) and after (right panel) L-tetanus for the]-stimulus (white bars) and the [-stimulus (black bars). (C) Distribution of the IntFR before (left panel) and after (right panel) L-tetanus for the]-stimulus (white bars) and the [-stimulus (black bars) for 4 different neuronal cultures. In the left panels the distributions of IntFR for the 2 stimuli are almost entirely overlapping. In the right panels, as consequence of LTP induction, the overlap of the distributions for the]-stimulus and [-stimulus is enormously decreased.

Given this decomposition, according to (2), the processing of an 8-bit image is obtained as

$$\sum_{p=1}^8 \alpha^{(p)} 2^{(p-1)} I_{ij}^{(p)} ** h(\rho, t) \quad (4)$$

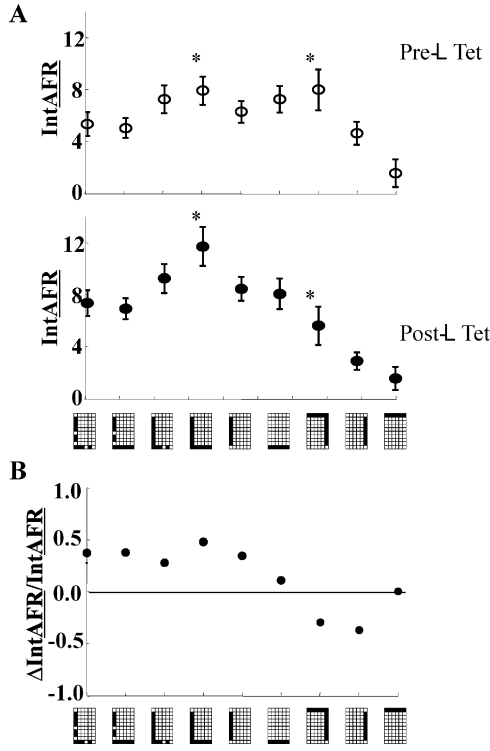


Fig. 7. Spatial selectivity of LTP. (A) Int.AFR before (open symbols) and after (filled symbols) [-tetanus for stimuli shown with the shape indicated in the abscissa. Int.AFR before and after tetanus was obtained as an average during 30 min before and after tetanus respectively. The voltage intensity of the stimulation was 0.6 V. Stars indicate the response to the [-stimulus and]-stimulus. (B) Relative change of the Int.AFR produced by the [-tetanus. Data obtained from those shown in A before and after [-tetanus.

where $\alpha^{(p)}$ is a scaling factor (see Section II). By processing independently the 8 1-bit images with the neuronal culture, a low or a bandpass filtering of an 8-bit image is obtained. A low-pass filtering of the original 8 bit images [Fig. 8(a) left panels], obtained by the neuronal culture in the time bin 1–6 ms and by a digital filtering with a Gaussian function, are shown in the central and right panels respectively of Fig. 8(a). The high similarity of images in the central and right panel shows that the proposed hybrid device can process efficiently 8 bit images. After a neuronal culture has learned, its temporal-spatial filtering is different. First of all, it is not anymore spatially invariant and, therefore, cannot be described by a temporal and spatial convolution as in (4). In fact, the firing rate $\text{FR}_{ij}(t)$ evoked by a given image I_{ij} cannot be predicted from (1) and (2) but must be measured. The processing of an 8-bit image is, therefore, obtained as

$$\sum_{p=1}^8 \alpha^{(p)} 2^{(p-1)} \text{FR}_{ij}^{(p)}(t) \quad (5)$$

where $\text{FR}_{ij}^{(p)}(t)$ is the measured response to $I_{ij}^{(p)}$ after tetanization and $\alpha^{(p)}$ is a scaling factor (see Section II). Having lost spatial invariance, the device is now able to extract a specific pattern from a complex image. When the neuronal culture has learned to recognize an [- [see Fig. 8(b)], the processing of original images [Fig. 8(b) left column] is modified [see central column of Fig. 8(b)] and becomes tuned and selective to [-stimulus [right column of Fig. 8(b)]. It is evident that after learning, the neu-

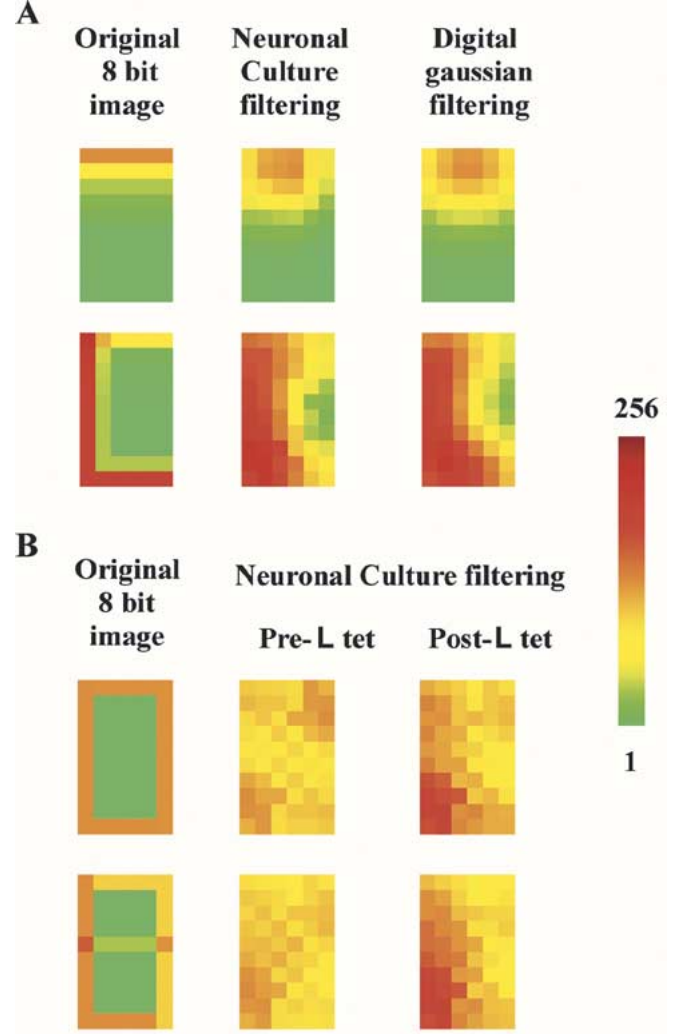


Fig. 8. Image processing of 8-bit images. (A) Low-pass filtering of two different 8-bit images. (Left panels) The original 8 bit images. (Central panels) Low-pass filtering of the images obtained with the neuronal culture. (Right panels) Low-pass filtering of the images, obtained by digital convolution of the original 8-bit image, with the Gaussian profile shown in 2A in the time window between 1 and 6 ms. Color-coding is reproduced at the right side of the figure. (B) Features extraction obtained by low-pass filtering of two different 8-bit images before and after learning. (Left columns) The original 8 bit images. (Central columns) Low-pass filtering of the images obtained with the neuronal culture before the tetanization. (Right columns) Low-pass filtering of the images obtained with the neuronal culture after [-tetanus. Color-coding is reproduced at the right side of the figure. Original 8-bit images are obtained according to (3). For 1-bit processed images, the values of the $\text{AFR}_{ij}(t)$ were scaled between 0 and 1 by dividing for the corresponding maximal value among all electrodes in the time-window of 1–30 ms. 8-bit processed images are then obtained by (4). For features extraction, the values of $\text{AFR}_{ij}(t)$ obtained after the tetanization were scaled by dividing for the same maximal value calculated before the tetanization. 8-bit processed images are then obtained by (5) (see Section II).

ronal culture is able to extract the [- from the rest of the image, in both processed images. The upper image shows clearly that, before learning, the neuronal filtering is symmetric and becomes asymmetric after learning, allowing, in this way, the extraction of the learned feature.

G. Consistency of Potentiation and Learning

Neural plasticity is certainly a major advantage for Neurocomputers if LTP or LTD can be evoked in a neuronal culture

consistently and in a repeated way. As shown by Jimbo *et al.* [23] when a tetanizing train of pulses is applied through a single electrode of a MEA both LTP and LTD can be observed. The induction of LTP occurred when neurons before tetanus fired in a correlated way; while LTD occurred when the firing of neurons were poorly correlated. Therefore, when a single electrode was used the induction of LTP or LTD could not be controlled but depended from the intrinsic connectivity of the network. This situation is not satisfactory if neuronal cultures have to be used for information processing and learning. Therefore, we looked for experimental conditions in which LTP could be induced consistently. LTP described in previous sections was always evoked when the same tetanizing pulse was applied to many electrodes, more than 10, with a spatial profile of two perpendicular bars. With this pattern of stimulation, LTP was successfully induced in 10 (over 12 tested) neuronal cultures. LTP could be evoked in the same neuronal culture on different days over a period of 6 weeks. When the tetanus was applied through a smaller number of electrodes, i.e., less than 7, LTP was not consistently induced and both LTP and LTD was observed. When a bar-tetanus was delivered, LTP was never induced in 6 experiments. In 3 experiments performed with young (less than 20 days) neuronal cultures, stimulation applied to a bar of electrodes, either horizontal or vertical, produced an electrical excitation confined around the electrodes used for stimulation, and LTP could not be induced by an \lfloor -tetanus. In one dish the two tetanization protocols were combined: a bar-tetanus was first applied and, after 2 hours, an \lfloor -tetanus was applied. The response to the \lfloor -stimulus after the bar-tetanus was unchanged, while the \lfloor -tetanus clearly induced LTP. LTP could be evoked in the same neuronal culture, on different days over a period of 6 weeks. When 50 micromolar DL-2-amino-5-phosphonovaleric acid (APV), a well known blocker of NMDA channels, was added to the extracellular medium bathing the neuronal culture, the evoked electrical activity did not spread significantly from the electrodes used for stimulation, as in cortical neuronal cultures [24]. Under these conditions LTP could not be induced in the neuronal cultures.

IV. DISCUSSION

The work described here demonstrates that, by growing neuronal cultures over multi electrode arrays (MEA), a new hybrid-computing device, composed of biological neurons and metal electrodes, can be foreseen. The biophysical mechanisms underlying the low-pass and band-pass filtering of digital images, here described, originate from membrane properties of cultivated neurons and their mode of interaction. Synaptic properties limit and shape the propagation of action potentials in the culture. The combination of these biophysical mechanisms determines the exact parameters of the filtering. The consistency of the experimental set up was discussed in the two sections on the reproducibility of neuronal filtering and consistency of potentiation and learning. The major difference with previous work on neuronal culture grown on MEA [23]–[25] is the controlled induction of LTP and its use for pattern recognition. The presented results, show, in our opinion, that neuronal cultures grown on MEA can constitute the basis for the development of Neurocomputers, possibly new computing devices.

A. Comparison With Previous Work

The present work is a continuation of previous analysis of the behavior of neuronal cultures grown on MEAs [23]–[25] and confirms several previous observations on how the evoked electrical activity spreads throughout the neuronal culture. Jimbo *et al.* [23] have shown that when a tetanizing train of pulses is applied through a single electrode of a MEA, both LTP and LTD can be observed and that the induction of LTP or LTD depended from the intrinsic connectivity of the network. The present work shows that, when many electrodes are used for tetanizing, LTP is preferentially induced and, therefore, the induction of LTP can be controlled. The controlled induction of LTP allows the use of neuronal cultures for pattern recognition (see Figs. 5 and 6) and opens the way for using neuronal cultures as new computing devices, i.e., Neurocomputers. Although the molecular mechanisms controlling the induction of LTP and/or LTD have not yet been fully revealed [26], it is well established that a moderate elevation of intracellular Ca^{2+} favors the induction of LTD, while a larger increase is more likely to induce LTP. As neuronal firing leads to an elevation of intracellular Ca^{2+} , it is not surprising that a massive electrical excitation preferably induces LTP instead of LTD. As stated in the Results section, LTP was induced in 10 over 12 tested neuronal cultures. However, in all neuronal cultures, after an \lfloor -tetanus, the discriminability between an \lfloor and \rfloor -stimulus increased. Therefore, in all tested cultures learning was observed, provided that the tetanus was applied through a sufficiently large number of electrodes. LTP was not observed when the frequency of tetanization was lower than 100 Hz.

B. Reproducibility and Reliability of Neuronal Firing

The reliability of the evoked response increases by pooling the electrical activity recorded from a larger number of neurons, as shown by the decrease of the $\text{CV}(t)$ calculated for a single electrode, a row of electrodes or the 60 electrodes of the MEA. These conclusions, drawn from an investigation in a dissociated culture of hippocampal neurons, are remarkably similar to those obtained in an isolated leech ganglion (5) and in a semi-intact leech [27]. In the leech nervous system, motoneurons coactivated during the same behavioral reaction, fire spikes in an almost statistically independent way. As a consequence of statistical independence pooling, the electrical activity over all co-activated motoneurons makes highly variable spike trains underlying reproducible motor reactions.

These results suggest that, analogously to nervous systems, reliability and reproducibility of neurocomputers can be obtained by pooling the neuronal electrical activity over populations of neurons, as already shown by several previous investigations with intelligent prostheses [28]–[31]. The extent of pooling depends on the task to be solved: in fact, when it is necessary to discriminate between patterns, it is convenient to average the neuronal activity over a very large number of neurons (of the order of 100) in order to obtain a successful discrimination over a single trial, as shown in Fig. 6. When the MEA is used to filter images, averaging is restricted to neurons recorded from the same electrode, i.e., less than 6 or so different neurons. In this case the resulting computation is noisier. In a population of N neurons firing spikes in an almost unrelated way, the CV decreases as the square root of N [32]. Therefore, if each neuron

has a CV between 0.5 and 1 [27], a good reproducibility – with a CV of less than 0.1 – can be obtained by pooling the electrical activity of 100–1000 neurons, i.e., the same order of magnitude of neurons thought to be present in a column in the cortex [33]. This requirement may pose severe constraints on the construction of MEA and on the development of future Neurocomputers.

C. Limitations of the Tested Device

The tested device, based on the MEA supplied by MultiChannelSystem, has several limitations, which may be overcome by future technological improvements. First of all, in the present release it is not possible to stimulate and record simultaneously from the same electrode, contrary to the MEA developed by Jimbo and coworkers [25]. As a consequence, the electrical activity evoked in the stimulated electrode cannot be measured but has to be interpolated (see Section II) from the neighboring recording electrodes. In addition, switching between recording and stimulation cannot be obtained via software and has to be performed manually, reducing the possible experimentation and the analysis of parallel processing with the neuronal culture. Recently new circuits for distributing stimuli to all electrodes electronically (from Multichannel Systems, MEA1060-BC) and for stimulating and recording on the same electrode [34] have been developed. These circuits will allow to overcome the limitations discussed above. The implementation of on-line analysis [21], [35] allows the exploration of alternative parallel processing and learning with the neuronal culture.

Another disadvantage of the present device, possibly shared by a large variety of Neurocomputers, is the presence of silent electrodes or of electrodes making good electrical contacts with a limited number of neurons. The ideal device is composed of electrodes all making good electrical contact with a large number of healthy neurons. Since it is necessary to measure individual spikes and not field potentials, the number of neurons in good electrical contact with each electrode cannot be too high. Therefore, it is necessary to develop standard protocols in order to have MEA with almost all electrodes making good electrical contact with approximately the same number of neurons.

The training procedure, by which a neurocomputer learns to recognize a spatial feature, is simply an appropriate tetanus, i.e., a relatively simple procedure, representing, therefore, an obvious advantage of the Neurocomputer. On the other side the Neurocomputer – at least in its present form – seems to be primarily a coprocessor, which cannot be easily programmed for a different task, as usual digital processor can. After the decline of LTP, the neurocomputer can be trained to learn a new pattern and, therefore, can be reprogrammed and becomes reusable. Several issues, however, must be addressed such as the duration of induced LTP, the possibility of encoding new inputs and to erase stored information – possibly by inducing LTD. Once these issues will be properly addressed, the exploitation of LTP, as here demonstrated, and of LTD [18], [36], may provide a natural implementation of algorithms based on artificial neural networks (ANN).

D. Future of Neurocomputers

The use of biological neurons as computing devices opens a new avenue in which computer science can capitalize on the expertise and technology of cell biology and genetic engineering.

Taking advantage of stem cell technology [37]–[39] we are trying to obtain a standard source of neurons in order to eliminate the variability intrinsic to individual rats, possibly leading to computing devices with a much higher reproducibility. Stem cell technology could provide also populations of neurons with specific properties, for example neurons that release selected neurotransmitters. In this way neuronal cultures with controlled ratios of inhibitory and excitatory neurons could be constructed. The possibility of guiding neuronal growth along specific spatial directions [40]–[43] will allow the fabrication of large variety of spatial filters, imitating the receptive field properties of neurons in early visual area [44]. Neurocomputers can become promising new computing devices if their reliability can be increased. In order to do so, besides using stem cell technology for obtaining a standardized source of neurons, it will be necessary to automate with appropriate robots all the subsequent procedures necessary for preparing and maintaining neuronal cultures. It will be very important to standardize the handling of MEAs, neuron deposition on the MEAs and their maintenance.

ACKNOWLEDGMENT

The authors would like to thank Dr. E. Cherubini and Dr. G. Musso for helpful comments and D. Dean for carefully reading the manuscript.

REFERENCES

- [1] D. Marr, *Vision: A Computational Investigation into the Human Representation and Processing of Visual Information*. San Francisco, CA: Freeman, 1982.
- [2] D. E. Rumelhart and J. L. McClelland, *Explorations in Parallel Distributed Processing*. Cambridge, MA: MIT Press, 1988.
- [3] J. G. Nicholls, B. G. Wallace, A. R. Martin, and P. A. Fuchs, *From Neuron to Brain: A Cellular and Molecular Approach to the Function of the Nervous System*, 4th ed. Sunderland, MA: Sinauer, 2000.
- [4] M. N. Shadlen and W. T. Newsome, "Noise, neural codes and cortical organization," *Curr. Opin. Neurobiol.*, vol. 4, pp. 569–579, 1994.
- [5] D. Zoccolan, G. Pinato, and V. Torre, "Highly variable spike trains underlie reproducible sensory-motor responses in the medicinal leech," *J. Neurosci.*, vol. 22, pp. 10 790–10 800, 2002.
- [6] J. Hertz, A. Krogh, and R. G. Palmer, "Introduction to the theory of neural computation," in *Studies in the Sciences of Complexity*. Santa Fe, NM: Santa Fe Institute, 1991, vol. 1.
- [7] J. J. Hopfield, "Neural networks and physical systems with emergent collective computational ability," *Proc. Nat. Acad. Sci.*, vol. 79, pp. 2554–2558, 1982.
- [8] M. Minsky and S. Papert, *Perceptrons: An Introduction to Computational Geometry*. Cambridge, MA: MIT Press, 1988.
- [9] G. W. Gross, E. Riesecke, G. W. Kreutzberg, and A. Meyer, "A new fixed-array multimicroelectrode system designed for long-term monitoring of extracellular single unit neuronal activity *in vitro*," *Neurosci. Lett.*, vol. 6, pp. 101–105, 1977.
- [10] J. Pine, "Recording action potentials from cultured neurons with extracellular microcircuit electrodes," *J. Neurosci. Meth.*, vol. 2, pp. 19–31, 1980.
- [11] J. L. Novak and B. C. Wheeler, "Recording from the aplysia abdominal ganglion with a planar microelectrode array," *IEEE Trans. Biomed. Eng.*, vol. BME-33, pp. 196–202, 1986.
- [12] Y. Jimbo and A. Kawana, "Electrical stimulation and recording from cultured neurons using a planar electrode array," *Bioelectrochem. Bioenergetics*, vol. 29, pp. 193–204, 1992.
- [13] S. Martinoia, M. Bove, G. Carlini, C. Ciccarelli, M. Grattarola, C. Stormont, and G. Kovacs, "A general purpose system for long-term recording from a microelectrode array coupled to excitable cells," *J. Neurosci. Meth.*, vol. 48, pp. 115–121, 1993.
- [14] S. Vassanelli and P. Fromherz, "Neurons from rat brain coupled to transistors," *Appl. Phys. A*, vol. 65, pp. 85–88, 1997.

- [15] G. Zeck and P. Fromherz, "Noninvasive neuroelectronic interfacing with synaptically connected snail neurons immobilized on a semiconductor chip," *Proc. Nat. Acad. Sci.*, vol. 98, pp. 10457–10462, 2001.
- [16] P. Bonifazi and P. Fromherz, "Silicon chip for electronic communication between nerve cells by noninvasive interfacing and analog-digital processing," *Advanced Mater.*, vol. 14, pp. 1190–1193, 2002.
- [17] T. V. P. Bliss and G. L. Collingridge, "A synaptic model of memory: Long-term potentiation in the hippocampus," *Nature*, vol. 361, pp. 31–39, 1993.
- [18] O. Paulsen and T. J. Sejnowski, "Natural patterns of activity and long-term synaptic plasticity," *Curr. Opin. Neurobiol.*, vol. 10, pp. 172–179, 2000.
- [19] S. M. Potter and T. B. DeMarse, "A new approach to neural cell culture for long-term studies," *J. Neurosci. Meth.*, vol. 110, pp. 17–24, 2001.
- [20] S. Marom and G. Shahaf, "Development, learning and memory in large random networks of cortical neurons: Lessons beyond anatomy," *Quart. Rev. Biophys.*, vol. 35, pp. 63–87, 2002.
- [21] G. Shahaf and S. Marom, "Learning in networks of cortical neurons," *J. Neurosci.*, vol. 21, pp. 8782–8788, 2001.
- [22] W. L. Ruten, "Selective electrical interfaces with the nervous system," *Annu. Rev. Biomed. Eng.*, vol. 4, pp. 407–452, 2002.
- [23] Y. Jimbo, T. Tateno, and H. Robinson, "Simultaneous induction of pathway-specific potentiation and depression in networks of cortical neurons," *Biophys. J.*, vol. 76, pp. 670–678, 1999.
- [24] Y. Jimbo, A. Kawana, P. Parodi, and V. Torre, "The dynamics of a neuronal culture of dissociated cortical neurons of neonatal rats," *Biol. Cybern.*, vol. 83, pp. 1–20, 2000.
- [25] Y. Jimbo, N. Kasai, K. Torimitsu, T. Tateno, and H. P. C. Robinson, "A system for MEA-based multisite stimulation. Biomedical engineering," *IEEE Trans. Biomed. Eng.*, vol. 50, no. 2, pp. 241–248, Feb 2003.
- [26] M. Sheng and M. J. Kim, "Postsynaptic signaling and plasticity mechanisms," *Science*, vol. 298, no. 5594, pp. 776–80, 2002.
- [27] I. Arisi, D. Zoccolan, and V. Torre, "Distributed motor pattern underlying whole-body shortening in the medicinal leech," *J. Neurophysiol.*, vol. 86, pp. 2475–2488, 2001.
- [28] J. Wessberg, C. R. Stambaugh, J. D. Kralik, P. D. Beck, M. Laubach, J. K. Chapin, J. Kim, S. J. Biggs, M. A. Srinivasan, and M. A. Nicolelis, "Real-time prediction of hand trajectory by ensembles of cortical neurons in primates," *Nature*, vol. 408, no. 6810, pp. 361–365, 2000.
- [29] M. A. Nicolelis, "Brain-machine interfaces to restore motor function and probe neural circuits," *Nat. Rev. Neurosci.*, vol. 4, no. 5, pp. 417–422, 2003.
- [30] A. E. Grumet, J. L. Wyatt Jr., and J. F. Rizzo, III, "Multi-electrode stimulation and recording in the isolated retina," *J. Neurosci. Meth.*, vol. 101, no. 1, pp. 31–42, 2000.
- [31] R. A. Normann, E. M. Maynard, P. J. Rousche, and D. J. Warren, "A neural interface for a cortical vision prosthesis," *Vis. Res.*, vol. 39, no. 15, pp. 2577–87, 1999.
- [32] A. Papoulis, *Probability, Random Variables and Stochastic Processes*. New York: McGraw-Hill, 1984.
- [33] V. B. Mountcastle, "The columnar organization of the neocortex," *Brain*, vol. 120, pp. 701–722, 1997.
- [34] D. A. Wagenaar and S. M. Potter, "A versatile all-channel stimulator for electrode arrays, with real-time control," *J. Neural Eng.*, vol. 1, pp. 39–45, 2004.
- [35] T. B. DeMarse, D. A. Wagenaar, A. W. Blau, and S. M. Potter, "The neurally controlled animat: Biological brains acting with simulated bodies," *Autonomous Robot.*, vol. 11, pp. 305–310, 2001.
- [36] D. J. Linden and J. A. Conner, "Long-term synaptic depression," *Ann. Rev. Neurosci.*, vol. 18, pp. 319–357, 1995.
- [37] T. Barberi, P. Klivenyi, N. Y. Calingasan, H. Lee, H. Kawamata, K. Loonam, A. L. Perrier, R. Bruses, M. E. Rubio, N. Topf, V. Tabar, N. L. Harrison, M. F. Beal, M. A. Moore, and L. Studer, "Neural subtype specification of fertilization and nuclear transfer embryonic stem cells and application in parkinsonian mice," *Nat. Biotechnol.*, vol. 21, pp. 1200–1207, 2003.
- [38] H. Kawasaki, H. Suemori, K. Mizuseki, K. Watanabe, F. Urano, H. Ichinose, M. Haruta, M. Takahashi, K. Yoshikawa, S. Nishikawa, N. Nakatsuji, and Y. Sasai, "Generation of dopaminergic neurons and pigmented epithelia from primate ES cells by stromal cell-derived inducing activity," *Proc. Nat. Acad. Sci.*, vol. 99, pp. 1580–1585, 2002.
- [39] J. J. Westmoreland, C. R. Hancock, and B. G. Condie, "Neuronal development of embryonic stem cells: A model of GABAergic neuron differentiation," *Biochem. Biophys. Res. Commun.*, vol. 284, pp. 674–680, 2001.
- [40] J. C. Chang, G. J. Brewer, and B. C. Wheeler, "Modulation of neural network activity by patterning," *Biosensors Bioelectron.*, vol. 16, pp. 527–533, 2001.
- [41] F. Nakamura, R. G. Kalb, and S. M. Strittmatter, "Molecular basis of semaphorin-mediated axon guidance," *J. Neurobiol.*, vol. 44, pp. 219–229, 2000.
- [42] J. A. Raper, "Semaphorins and their receptors in vertebrates and invertebrates," *Curr. Opin. Neurobiol.*, vol. 10, pp. 88–94, 2000.
- [43] M. Tessier-Lavigne and C. S. Goodman, "The molecular biology of axon guidance," *Science*, vol. 274, pp. 1123–1133, 1996.
- [44] D. H. Hubel and T. N. Wiesel, "Early exploration of the visual cortex," *Neuron*, vol. 20, pp. 401–412, 1998.



Maria Elisabetta Ruaro received the Laurea degree in biological science from the University of Trieste, Trieste, Italy, in 1984.

In 1987, she worked at the EMBL in Heidelberg in the group of Lennard Philipson, where she learned different cell biology and molecular biology techniques. From 1991 to 1997, she was responsible for the microinjection facility at the ICGEB-UNIDO at the Area Science Park while maintaining scientific collaboration with scientific groups in Italy, U.K., and USA. From 1998 to 2000, she was a Scientific

Collaborator at the LNCIB, where she studied two growth arrest specific genes Gas1 and Gas6, and became an expert in cell culture of different cell type and cell biology techniques. Since 2001, she has been a Research Fellow in the group of V. Torre at the International School for Advanced Studies where she participated to the neurocomputer project in particular to the cell culture and electrophysiological aspects. During this period she visited the laboratory of Dr. Studer at the Sloan Kettering Institute in New York where she learned the methodology to differentiate neurons from embryonic stem cells. Since 1996 she has been teaching cell biology, as an external teacher, at the University of Udine (IT) and Trieste (IT).



Paolo Bonifazi was born in Sassoferrato, Italy, in 1975. He received the Laurea degree in physics from the University of Perugia, Perugia, Italy, in May 2001. He is currently working toward the Ph.D. degree in neurobiology at the International School for Advanced Studies (ISAS/SISSA), Trieste, Italy. From January 2000 to July 2001, he was a trainee and a postgraduate student at the department of "Membrane and Neurophysics" of the Max-Planck-Institute for Biochemistry in Munich, under the supervision of Prof. P. Fromherz.

His research interests include electrophysiology, neuroengineering, computational neuroscience.



Vincent Torre received the degree in theoretical physics from Genoa University, Genoa, Italy, in 1973.

In the early 1980s, along with T. Poggio and C. Koch, he pioneered in the area of computational neuroscience. For several years he was a Post Doc and Visiting Scientist in Sir Alan Hodgkin Lab, Cambridge, U.K., where he learned a variety of electrophysiological methods and became expert in modeling biological process. In the late 1980s and early 1990s he worked on computer vision and in

particular, edge detection and motion perception. Since 1997 he has been a Full Professor at International School of Advanced Studies, Trieste, Italy and is the Head of the Department of Neurobiology. He has a well-established expertise in electrophysiology, computer vision, computational neuroscience and modeling biological process. He is the author of more than 100 full papers.